ULUSLARARASI 3B YAZICI TEKNOLOJİLERİ
VE DİJİTAL ENDÜSTRİ DERGİSİ
INTERNATIONAL JOURNAL OF 3D PRINTING
TECHNOLOGIES AND DIGITAL INDUSTRY

ISSN:2602-3350 (Online)
URL: https://dergipark.org.tr/ij3dptdi

OPTIMIZATION OF ANNEALING AND 3D PRINTING PROCESS PARAMETERS OF PLA PARTS

Yazarlar (Authors): Mhd Usama Alabd*, Abdurrahim Temiz

Bu makaleye şu şekilde atıfta bulunabilirsiniz (To cite to this article): *Alabd M. U., Temiz A., "Optimization of Annealing and 3D Printing Process Parameters of Pla Parts" Int. J. of 3D Printing Tech. Dig. Ind., 8(2): 185-201, (2024).*

DOI: 10.46519/ij3dptdi.1451666

Araştırma Makale/ Research Article

Erişim Linki: (To link to this article): https://dergipark.org.tr/en/pub/ij3dptdi/archive

OPTIMIZATION OF ANNEALING AND 3D PRINTING PROCESS PARAMETERS OF PLA PARTS

Mhd Usama Alabd[a]*, Abdurrahim Temiz[a]

[a]Karabük University, Technology Faculty, Industrial Design Engineering Department, TURKEY

* *Corresponding Author:* osama.alabd9994@gmail.com

(**Received:** 12.03.24; **Revised:** 24.06.24; **Accepted:** 09.08.24)

ABSTRACT

Fused Filament Fabrication (FFF) has gained significant popularity as the prevalent additive manufacturing method due to its ability to reduce production time and expenses. However, the constraints of limited dimensional precision, poor surface quality, and relatively low Ultimate Tensile Strength (UTS) hinder compliance with the stringent regulatory norms of conventional manufacturing, necessitating post-processing for enhancement. In this investigation, the response surface method was used to optimize annealing and specific printing parameters to enhance the quality of PLA parts produced by FFF. Tensile specimens were printed with varying production parameters and annealed at varying heat treatment parameters. The following parameters are specified: layer height (0.1, 0.2, and 0.3 mm), build orientation (0°, 22.5°, 45°, 67.5°, and 90°), annealing temperature (70, 90, 110, and 130 ºC), and annealing time (60, 120, 180, and 240 min). The optimization technique aimed to enhance the UTS and match the CAD dimensions while minimizing surface roughness. The RSM optimization analysis identified the optimal parameters as layer height of 0.1 mm, build orientation at 0 degrees, annealing temperature of 110 degrees, and annealing time of 180 min. The consistent achievement of high levels of agreement between estimated and experimental response values substantiates the proposed models. A composite desirability value of 0.80 was derived for the variables due to the optimization investigation.

Keywords: Additive manufacturing, Annealing, Response surface method, Optimization, 3D printing.

1. INTRODUTION

The novel technological process of additive manufacturing makes physical objects from digital 3D models generated through computer-aided design (CAD) [1]. The FFF is a highly prevalent approach in 3D printing fields. It involves the sequential deposition of layers to fabricate three-dimensional structures, utilizing thermoplastic materials as the primary medium [2-3]. The FFF technique has demonstrated its utility not only in the realm of prototype but also in the domain of industrial production, establishing itself as a multifaceted and invaluable way of manufacturing [4]. The precision, consistency, and range of materials utilized in 3D printing techniques, such as FFF, have advanced to a level suitable for implementation in industrial manufacturing technology [5]. The materials employed in FFF commonly consist of polylactic acid (PLA) [6]. This technique is renowned for its capacity to manufacture end-use components, rather than solely prototypes [6-7]. Nevertheless, the FFF technique is a multifaceted procedure that is subject to numerous factors that might impact the overall quality of the printed output [8-9].

The layer height in FFF has a notable impact on the printed parts' ultimate tensile strength, surface roughness, and dimensional accuracy. The effect of layer height on the mechanical characteristics of FFF-printed components has been the subject of several investigations. For instance, Rajpurohit and Dave varied the line width and height of the layers to study their effect on the tensile strength of PLA-printed parts. It was found that the layer height and line width substantially affected the tensile strength of the printed parts [10]. Similarly, Magri et al. highlighted that process settings, including

raster orientation, printing speed, and layer height significantly affect the tensile strength of FFF printed parts [11]. Furthermore, Vyavahare et al. concluded that as the height of a layer increases, its tensile strength diminishes, indicating a clear relationship between layer height and mechanical properties [12]. In addition to tensile strength, the layer height also influences surface roughness and dimensional accuracy. Hua et al. noted that FFF parts printed with lower layer heights exhibit better mechanical performance [13]. Moreover, Vyavahare et al. identified layer height and print speed as significant parameters for the dimensional accuracy of FFF parts [14]. Furthermore, Chohan & Singh found that electroplating on FFF parts enhanced tensile strength and surface finish, indicating the interplay between layer thickness and surface characteristics [15].

The build orientation in FFF also significantly influences the printed parts' surface roughness, mechanical characteristics, and dimensional accuracy. Several studies have investigated the impact of build orientation on the characteristics of FFF-printed parts. For instance, Syrlybayev et al. extensively reviewed the effects of various process settings, including build orientation, on the mechanical characteristics of FFF-printed parts. Their review highlighted the critical influence of build orientation on the strength properties of FFF-printed parts [16]. Similarly, Dey & Yodo found that specific build orientations and raster orientations were crucial for achieving optimum surface roughness in FFF-printed parts [17]. Furthermore, Singh et al. revealed that build orientation significantly impacts the ultimate tensile properties of the printed parts [18]. This underscores the importance of considering build orientation when optimizing the mechanical characteristics of FFF-printed parts. Additionally, Huang et al. emphasized build orientation as a critical factor affecting the quality of the part [19]. In addition to mechanical properties, build orientation also affects surface roughness and dimensional accuracy. Hervan et al. highlighted that part build orientation and other settings affect the flexural, tensile, and impact strength of FFF-printed parts [20]. Moreover, Eryildiz demonstrated that build orientation substantially impacted the printing time and tensile properties of FFF-printed parts [21]. This further emphasizes the multifaceted influence of build orientation on the overall quality of FFF-printed parts.

Furthermore, research has shown that adding heat treatment can influence FFF printed parts mechanical strength [22]. The process of annealing in FFF has a noticeably impact on the surface roughness, mechanical characteristics, and dimensional precision of the printed parts. Akhoundi et al. investigated the impact of annealing and nozzle temperature on the mechanical characteristics of high temperature PLA in FFF. Their study provides the impact of annealing on the mechanical behavior of FFF parts [23]. Torres et al. explored the effects of annealing on the roughness of the surface and tensile characteristics of FFF-printed ABS components. The study emphasized the critical aspects of concern pertaining to the annealing treatment, particularly focusing on time and temperature and its influence on quality of the printed parts [24]. Additionally, Shbanah et al. found that heat treatment, specifically annealing, led to a significant increase in the ultimate tensile strength (UTS) of FFF-printed PLA polymer specimens, highlighting the positive effect of annealing on mechanical properties [25]. Furthermore, Rane et al. investigated the effects of annealing on the UTS of parts printed using FFF. Their research sheds light on the impact of thermal annealing on the mechanical properties of FFF-printed parts, offering significant perspectives on the role of annealing in enhancing the mechanical performance of printed components [26]. Overall, annealing, layer height, and build orientation in FFF play an important role in determining the printed parts' ultimate tensile strength, roughness of the surface, and dimensional precision. Understanding the impact of annealing, layer height, and build orientation on these properties is essential for optimizing the FFF process parameters to attain the intended mechanical and dimensional characteristics of the parts.

The response surface methodology (RSM) can be utilized to optimize printing parameters and annealing conditions, aiming to boost the quality of printed parts [3]. Elkaseer et al. (2020) examined the impact of process parameters and their interrelationships on the resource efficiency and quality of the FFF printing method. The authors highlighted the possible utility of RSM in the optimization of

3D printing parameter values [27]. Magri et al. (2020) presented a three-dimensional response surface to figure out the target response values and comprehend the interplay of printing settings, demonstrating the efficacy of RSM in optimizing printing parameters [28]. Additionally, Ouassil et al. utilized RSM to optimize FFF parameters to boost mechanical characteristics, highlighting the role of RSM in enhancing the mechanical performance of can ultimately gain valuable insights into the complex interactions between printing parameters and annealing conditions. Leading to the enhancement of printing processes and the quality of printed components.

This study aims to assess the impact of various printing parameters, including layer height and structure orientation, as well as annealing heat treatment parameters, including annealing temperature and annealing time, on the printed parts [29]. Furthermore, Tho employed RSM to identify the ideal settings for FFF printed parts, showcasing the versatility of RSM in optimizing various aspects of the 3D printing process [30]. The application of RSM for 3D printing process parameters and annealing parameters offers a systematic and efficient approach to optimize the quality, mechanical properties, and resource efficiency of 3D-printed parts. By leveraging RSM, researchers mechanical characteristic, surface roughness, and dimensional precision of PLA components printed using FFF. The RSM was employed to optimize the experimental settings, while the Analysis of Variance (ANOVA) test was utilized to examine the results. The study's originality is shown by its evaluation of printer process parameters in conjunction with annealing heat treatment parameters and optimization of these parameters using RSM.

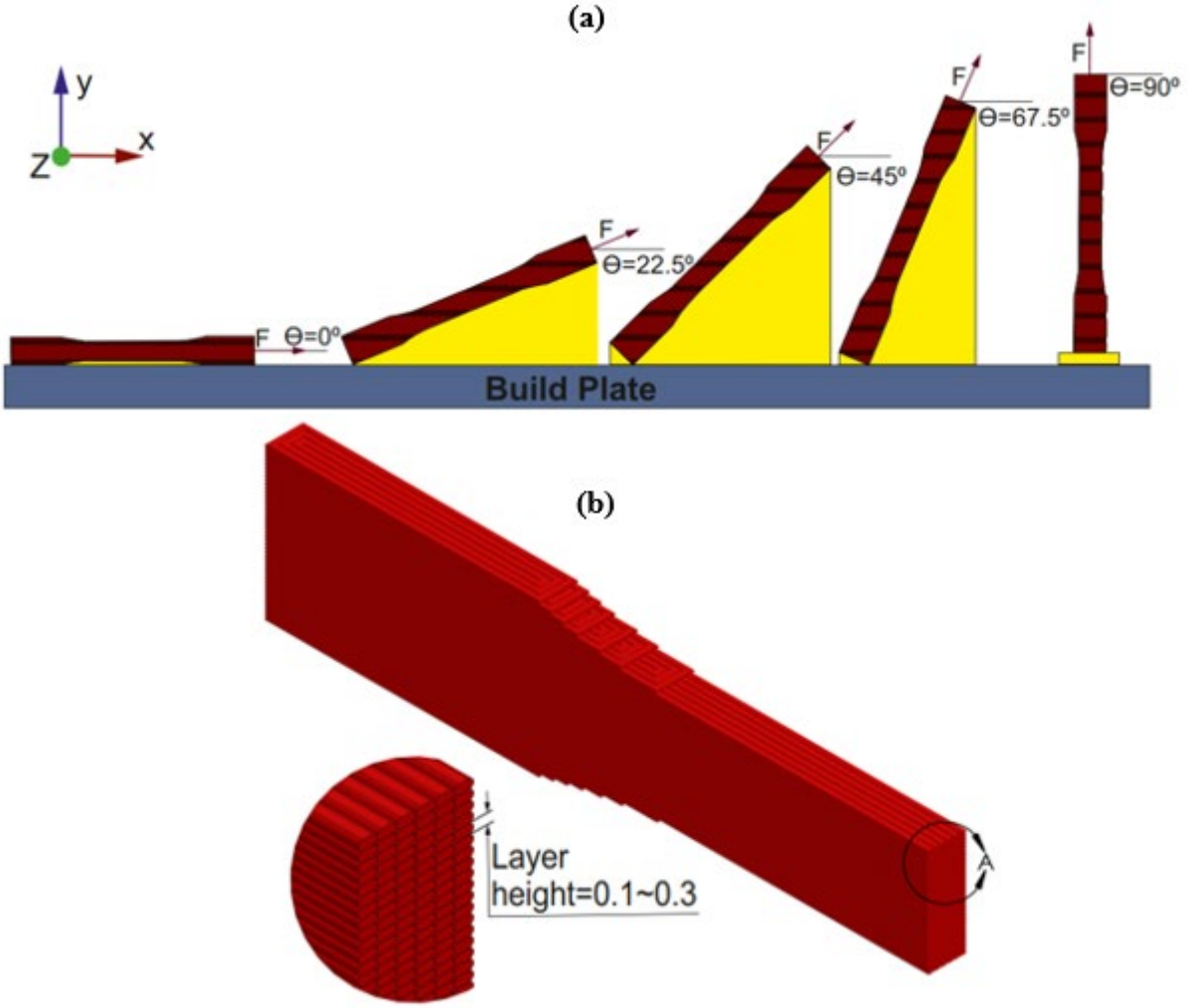

Figure 1. (a) The build orientations of the test specimens, and (b) the height of the layers.

2. MATERIALS AND METHODS

2.1. Specifications for printing and printers

All of the specimens utilized in this research were manufactured from PLA material by the FFF method, printed with a build volume of 200 × 200 × 220 mm on a cartesian type Zaxe X1 FFF 3D printer. The following 3D printing settings were utilized during the research: nozzle diameter of 0.4 mm, nozzle temperature of 215 °C, print speed of 70 mm/s, infill density of 100%, and bed temperature of 60 °C. A dog bone-shaped specimen was created to perform a tensile test with the purpose of assessing the tensile characteristics, dimensional precision, and surface roughness of plastic materials. Specimen dimensions were settled upon by consulting the ASTM Type I model [31], and the CAD model was created within the SolidWorks software environment. The print parameters used in this study were kept constant excluding the build orientation and layer height. The doge-bone tensile specimens were printed using various angles (0°, 22.5°, 45°, 67.5°, and 90°) and three-layer heights (1 mm, 2 mm, and 3 mm), as displayed in Figure 1. The entirety of the printed components was made with a density of 100% infill. The procedure makes use of a number of materials, although PLA is among the most used [6-7]. The PLA filament, with its properties clearly documented in [9], produced by ESUN, was used.

2.2. Annealing

Following the printing of the specimens, annealing is performed in accordance with the experimental design matrix. The processes of thermal annealing were carried out in a hot air oven. Four distinct temperatures (70, 90, 110, and 130 ◦C) and four distinct periods (60, 120, 180, and 240 min) were taken into account for the annealing process. Following the completion of the annealing procedure, the specimen remains within the oven until it reaches the ambient temperature.

2.3. Mechanical testing

The application of various criteria obtained from the DOE resulted in the effective production of a total of twenty-six distinct samples. A tensile test was conducted using the AG-50 kN Shimadzu Autograph. The test was carried out under standardized conditions, with a crosshead speed of 5 mm/min and at ambient temperature. Tensile testing was conducted following the recommendations presented in ASTM D638 [31]. The specimens underwent tensile testing until they reached the point of fracture. To minimize the influence of fluctuations and unpredictable inaccuracies, every recorded value in the dataset is based on a minimum of three valid tests. Throughout the experiment, no instances were observed where the samples exhibited any additional peaks in strength. Consequently, the UTS was identified as the highest stress value ever recorded.

2.4. Dimensional accuracy

The gauge section of the dog-bone tensile test specimen is of the utmost significance. Measurements were performed on dog bone samples at specified locations, including both ends and the middle (a total of three positions), as depicted in Figure 2 using digital vernier caliper. The objective was to independently assess the accuracy and precision of both thickness (h) and width (b). Therefore, in order to assess the precision, it was necessary to compare the produced dimensions with the original CAD design. Through the use of the standard deviation calculations, the precision (consistency) was defined. The weight of all samples was measured, and their accuracy was confirmed as well.

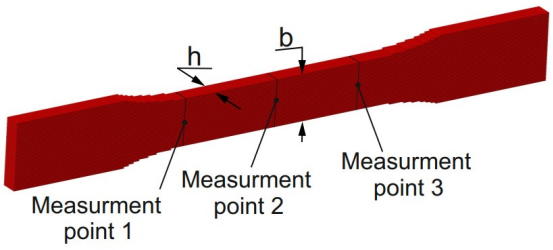

Figure 2. The schematic representation of measurement sites for width (b) and thickness (h) on the gauge section of the dog-bone specimen.

2.5. Surface Roughness

The surface finish quality of a component is related to its measured roughness. Roughness refers to the extent to which the chosen process parameters result in the appearance of surface irregularities on the printed object. Prior research has shown that components generated using the FFF process exhibit increased surface

roughness values, indicating a below-average surface quality [32]. Determining the effect of various printing settings on the surface roughness of the samples is a complex and challenging task. As a result, measurements were performed in two separate directions, specifically Vertical and Horizontal, relative to the tensile direction of the test specimen utilized in the tensile test. This is illustrated in figure 3, which serves as a schematic representation of the surface roughness measurements. The inability to measure perpendicular to the printing direction solely arises from the fact that the printing direction serves as a printing parameter, causing a shift in the orientation of each sample. The roughness measurements were performed using the Mitutoyo Surftest SJ-210, a needle-tipped inductive roughness device. The Mitutoyo SJ-210 table surface tester, equipped with a 20-millimeter-long probe, allows for effortless inspection of surfaces. The tester's stylus tip has a radius of 2 µm, while its detecting force amounts to 4 mN. The measurement of surface roughness was conducted with a "cut-off length" of 0.8 mm in the Z-axis orientation. Every evaluation condition was executed a minimum of five times on distinct areas of the FFF 3D printed objects' surfaces to ensure that the results obtained can be replicated. In order to properly evaluate the results, just one result was obtained by calculating the arithmetic mean.

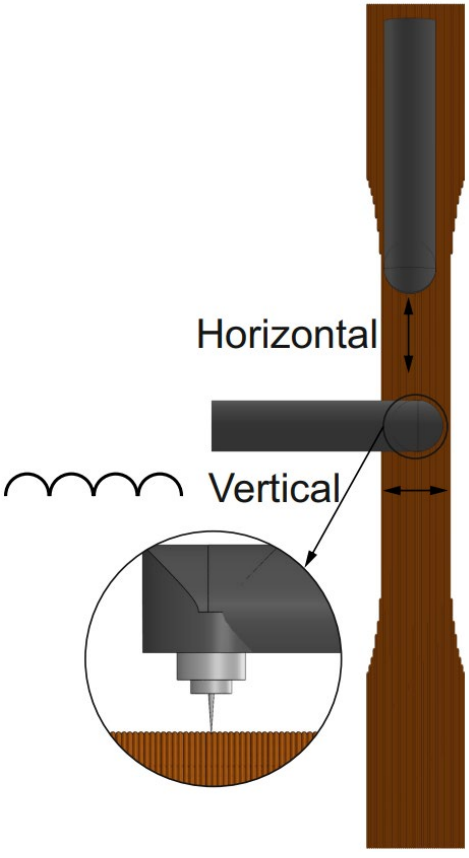

Figure 3. A schematic representation of the surface roughness measurements.

2.6. Response Surface Method

The printed components are affected by several processing parameters, such as layer height and build orientation [15,16]. The quality of components is affected by a number of variables, including the annealing parameters and the printing parameters. Specifically, the annealing temperature and the exposure period to this temperature perform a key role in deciding the components' quality [21,23]. The criteria for factor selection are established based on the extant literature and the corresponding degrees of importance attributed to each. The aim of this investigation was to assess the printing and annealing parameters of FFF-printed items. An insufficient amount of scholarly research has been devoted to the comprehensive evaluation of surface roughness, mechanical properties, and dimensional precision of heat-treated objects produced via FFF technology. This situation requires a substantial amount of tests. The objective of optimization is to optimize specific variables by either maximizing, minimizing, or reaching a target value, while also adhering to stated constraints, in order to get the most optimal outcomes. The utilization of RSM, a widely used technique, appears to offer benefits in the creation of an effective approximation method [33]. RSM is a powerful optimization tool that combines mathematical statistics to model both input and output parameters. As a result, one can determine the important elements and their respective amounts while also determining the best experimental conditions [34]. The use of RSM in this study is justified because several input and output factors are present.

A primary goal of optimization is to enhance the UTS while also minimizing surface roughness and achieving the desired CAD dimensions. The purpose of this optimization is illustrated in figure 4

Response	Goal	Lower	Target	Upper	Weight	Importance
Ra(V) (µm)	Minimize	1,04	1,04	24,35633333333	1	1
Ra(H) (µm)	Minimize	0,837666666666	0,837666666666	23,18	1	1
b (mm)	Target	12,64444444444	13	13,90444444444	1	1
h (mm)	Target	3,166666666666	3,2	3,707777777777	1	1
UTS (Mpa)	Maximize	9,3149	58,6939	58,6939	1	1

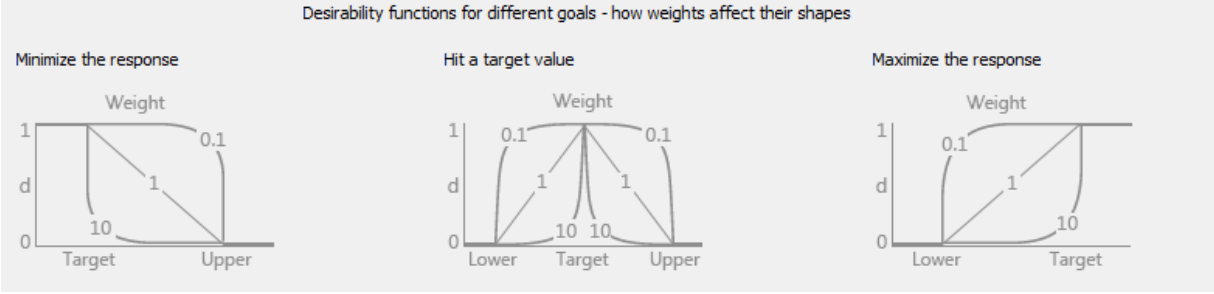

Figure 4. Different optimization goals and objectives correspond to distinct desirable functions.

The relevant experimental study was developed using Minitab, an RSM-based program. Each input parameter is assumed to be calculable and can be expressed as follows within the context of RSM [35].

$$y = F(x_1, x_2, \dots, x_m) \quad (1)$$

In the above situation, the variables x_1, x_2, ..., x_m, and y indicate the input and output factors, respectively. Within the framework of RSM, the primary phase entails establishing a robust connection between the two variables. The connection is clarified by employing a model based on second-order equations [35].

$$y = b_0 + \sum_{i=1}^{m} b_i x_i + \sum_{i=1}^{m-1} \sum_{j \geq i}^{m} b_{ij} x_i x_j + \sum_{i=1}^{m} b_{ii} x_i^2 + \varepsilon \quad (2)$$

The equation provided indicates the linear coefficient (i), the coefficient for the second order term (j), the regression coefficient (b), the total number of parameters (m), and the error associated with the response variable (ε). It is recommended to utilize RSM to investigate three dependent responses and three independent variables (one of which is a categorical factor and two of which are continuous factors) with a total of 26 experiments. Surface roughness, dimensional accuracy, and UTS are the output factors chosen for the settled RSM model. However, considering the model is configured with the following input parameters: build orientation, layer height, and annealing parameters (temperature and time). The annealing parameters, time and temperature are interdependent categorical factors. On the other hand, the printing parameters, layer height, and build orientation are continuous parameters. All other printing and post-processing factors that could affect printed component quality are kept constant.

3.RESULTS AND DISCUSSIONS

The present part examines and analyzes the outcomes of tensile testing, specifically focusing on the impact of layer height, build orientation, and annealing process parameters (time and temperature) on ultimate tensile strength (UTS). Table 1 presents the design table, which contains data from 26 tests and their corresponding responses.

Table 1. The values of the experimental response variable and the experimental design matrix.

Run Order	Layer Height, mm	Build Orient-ation, °	Temperature,°C -Time, min	UTS, Mpa (± SD)	h, mm (± SD)	b, mm (± SD)	Ra(H), µm (± SD)	Ra(V), µm (± SD)
1	0.1	0	0-0	54.65±0.7	3.17±0.02	13.43±0.04	0.95±0.16	7.46±0.3
2	0.1	22.5	70-60	46.31±0.7	3.28±0.02	13.54±0.14	8.04±0.15	8.41±0.24
3	0.1	67.5	110-240	18.96±1.4	3.34±0.03	12.78±0.08	8.71±0.77	7.72±1.04
4	0.1	90	130-120	10.99±1.1	3.28±0.03	12.64±0.08	9.16±1.07	2.60±1.7
5	0.1	0	70-240	58.69±0.5	3.17±0.01	13.90±0.04	1.16±0.27	10.57±0.4
6	0.1	22.5	130-60	45.78±1.6	3.35±0.04	13.51±0.09	8.20±0.13	9.99±1.26
7	0.1	67.5	90-240	19.64±1.8	3.27±0.04	12.78±0.07	8.13±0.27	7.74±0.03
8	0.1	90	0-0	38.65±2	3.28±0.03	12.96±0.02	7.88±0.28	2.29±0.12
9	0.2	0	90-120	52.88±0.4	3.25±0.03	13.62±0.05	1.11±0.25	14.87±0.42
10	0.2	22.5	110-240	37.52±6.9	3.44±0.06	13.43±0.2	11.74±0.84	14.41±0.99
11	0.2	45	0-0	38.76±1.6	3.54±0.03	13.39±0.07	14.94±0.39	14.56±0.46
12	0.2	67.5	130-180	24.93±1	3.53±0.05	13.10±0.12	14.94±0.53	12.04±0.8
13	0.2	0	110-60	53.89±0.2	3.31±0.04	13.66±0.06	1.22±0.29	14.86±0.29
14	0.2	22.5	0-0	50.42±1	3.38±0.02	13.46±0.09	12.31±1.44	14.85±0.28
15	0.2	45	70-120	28.43±2.9	3.47±0.03	13.33±0.04	14.62±0.19	14.53±0.19
16	0.2	67.5	130-240	18.53±1.4	3.46±0.04	13.10±0.05	14.55±0.18	11.67±0.46
17	0.2	90	90-120	32.13±0.3	3.56±0.06	13.17±0.06	14.98±0.19	1.81±0.32
18	0.3	0	130-180	42.28±2.3	3.27±0.03	13.45±0.09	1.87±0.45	24.36±0.56
19	0.3	22.5	90-60	45.03±2.1	3.50±0.04	13.68±0.07	12.58±2.08	22.87±1.82
20	0.3	90	110-120	9.31±1.9	3.70±0.07	13.28±0.06	22.95±0.46	1.25±0.22
21	0.3	0	90-180	43.61±1.3	3.24±0.04	13.51±0.07	0.84±0.11	24.13±1.37
22	0.3	22.5	0-0	41.88±3.83	3.42±0.03	13.45±0.03	13.11±1.3	22.85±0.58
23	0.3	45	130-60	26.81±0.9	3.61±0.07	13.56±0.12	20.89±0.49	19.91±0.35
24	0.3	67.5	70-240	24.52±0.6	3.71±0.05	13.29±0.05	22.88±0.72	12.92±1.33
25	0.3	90	130-240	16.7±3.1	3.67±0.07	13.32±0.05	23.18±0.8	1.04±0.31
26	0.3	0	110-180	50.92±1	3.37±0.02	13.48±0.01	1.08±0.32	22.54±0.63

It also analyzes the influence of these factors on surface roughness and dimensional precision. Variance analysis can be employed to derive numerical data pertaining to the probability value. ANOVA can accurately predict the optimal combination of process variables and identify the main contributing factors. Models with a p-value larger than 0.05 are widely regarded as insignificant. The resulting model is significantly influenced when a factor's p-value is less than 0.05 [33]. The ANOVA results in Table 2 indicate that all of the p-values for the linear coefficients of the build orientation are below 0.05. All the p-values for the linear coefficients of layer height are below 0.05, except for UTS. All p-values for the linear coefficients of the categorical factor temperature-time are greater than 0.05 for dimensional precision and surface roughness measured in the vertical direction. However, p-values are less than 0.05 for UTS and surface roughness measured in the horizontal direction. The p-values for layer height and build orientation, in relation to UTS and surface roughness, are less than 0.05, except for surface roughness measured vertically. However, the p-values for layer height and build orientation are greater than 0.05 for dimensional precision and surface roughness measured horizontally. In the case of 2-way Interaction, the p value is over 0.05 for UTS and b, and below 0.05 for surface roughness and h. The significance of the term in the proposed correlations of response becomes more pronounced as the p value decreases and f value increases. The primary factor that significantly affects all responses is the build

orientation, as evidenced by the ANOVA table. Furthermore, it is seen that the categorical variable of time-temperature has a greater impact on the UTS compared to the layer height. Conversely, the opposite holds true for surface roughness and dimensional correctness.

Table 2. Results of ANOVA include the p value, f value, and R2 value.

	UTS (MPa)		h (mm)		b (mm)		Ra(H)		Ra(V)	
	F value	P value	F value	P value	F value	P value	F value	P value	F value	P value
Model	22.90	0.001	28.05	0.001	6.87	0.021	161.00	0.000	39.84	0.000
Linear	25.48	0.001	26.39	0.001	6.98	0.021	129.60	0.000	34.77	0.000
X-Layer height	1.77	0.241	93.04	0.000	6.68	0.049	420.41	0.000	31.86	0.002
Y-Build orientation	62.12	0.001	126.36	0.000	19.86	0.007	690.26	0.000	166.30	0.000
CT-Temperature-Time	5.88	0.030	1.84	0.260	1.25	0.433	5.74	0.032	1.13	0.484
Square	5.96	0.047	12.56	0.011	2.38	0.188	59.02	0.000	18.82	0.005
X^2	6.99	0.046	2.72	0.160	4.31	0.093	15.89	0.010	0.69	0.443
Y^2	11.90	0.018	2.56	0.170	4.21	0.096	9.33	0.028	19.25	0.007
2-Way Interaction	0.36	0.576	25.47	0.004	0.68	0.446	91.30	0.000	35.04	0.002
X*Y	0.36	0.576	25.47	0.004	0.68	0.446	91.30	0.000	35.04	0.002
R^2, %	98.92%		99.12%		96.49%		99.84%		99.38%	
Adj. R^2, %	94.60%		95.58%		82.44%		99.22%		96.88%	

The influence of printer parameters (specifically, build direction and thickness of layers) in conjunction with annealing process parameters on the UTS result is illustrated in Figure 5. The results indicated a negative relationship between the UTS and the increase in layer thickness without any post-processing. The decrease in UTS found when the thickness of layers in 3D printed parts increases, without any post-processing, can be due to many variables that have been explained in the existing literature. An extensive study has been conducted on the correlation between layer height and the UTS of 3D printed components. Hua et al. (2023) noted that FFF specimens printed with lower layer heights exhibit better mechanical performance [13]. Choudhary et al. [36] also discovered an inverse interaction between layer thickness and the decrease in UTS. Furthermore, it was noted that decreasing the layer height resulted in a higher level of bonding, perhaps leading to an enhanced UTS [37]. It is observed that the UTS value exhibits a decreasing trend initially and subsequently rises with increasing layer thickness, owing to the thermal diffusion features [38]. These findings indicate that the thermal characteristics related to varying layer thicknesses can impact the bonding between layers and the overall structural strength of the printed objects. Grasso et al. [39] revealed a significant correlation between stiffness and strength, which was influenced by the infill orientation and temperature values. This indicates that the mechanical characteristic are affected by the printing parameters. Figure 5 demonstrates that in the samples without post-processing, the UTS initially drops and subsequently stabilizes as the structural orientation increases. The stability of the UTS can also be influenced by the variability in the height of each layer. The scholarly literature provides clarification on the phenomenon under consideration by employing the terms interlayer fracture and intralayer fracture [40]. The UTS results of annealed heat-treated samples varied depending on the printing parameters. Upon analysis of the sample with a layer thickness of 0.1 mm and a printing angle of 0°, it was seen that the sample, which underwent heat treatment at 70° C for 240 minutes, had a tensile strength roughly 10% higher than the untreated sample. The value shown represents the maximum UTS achieved in the experiments. A decrease in UTS is observed, particularly at a construct orientation of 90°, despite alterations to the annealing process parameters, as indicated by the graph. The UTS is significantly decreased by the

annealing heat treatment at 130°, and this reduction becomes more noticeable with longer durations. During the annealing heat treatment process at temperatures of 90° and 70°, it can be observed that the ultimate tensile strength (UTS) generally increases with longer durations. Nevertheless, establishing a universal correlation is not possible because to variations in layer thickness and build orientation. The ultimate tensile strength (UTS) of samples produced by FFF printing is influenced by the level of crystallinity in the printed object. The non-linear changes in UTS values can be attributed to the temperature-dependent modification of crystallinity during the printing process [41].

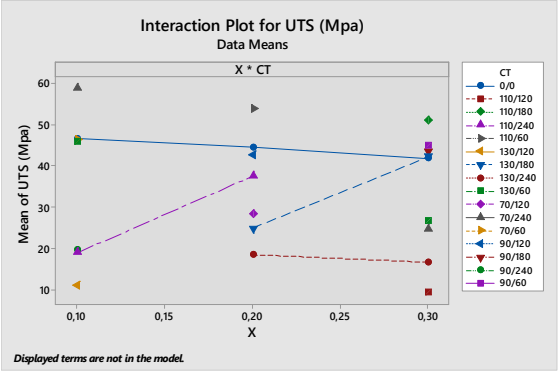

(a)

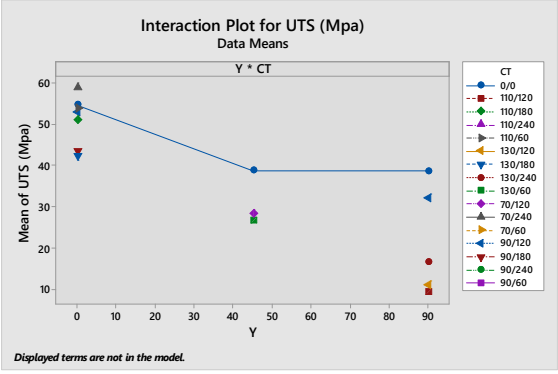

(b)

Figure 5. The surface roughness interaction plot with layer height, build orientation, and annealing parameters.

The correlation between printer parameters and annealing process parameters as they pertain to the surface roughness outcome is visually represented in Figure 6. Consistent with expectations, the samples utilizing the identical direction of printing and measurement exhibited the lowest surface roughness values. Conversely, as the angle between the printing orientation and the direction of measurement increased, the surface roughness value increased as well, reaching its maximum value in the fully perpendicular measurement. As mentioned in the literature [16,18], it was found that specific build orientations and raster orientations were crucial for achieving optimum surface roughness in FFF-printed parts. As expected, the graphs clearly indicate that altering the height of the layers has no effect on the roughness of the surface when the direction of measurement and the direction of printing are identical. However, when the orientation of printing and the direction of measurement were at at 90 degrees to each other, the roughness exhibited an upward trend with increasing layer height. This rise is roughly similar to the rate of increase in layer height. Several studies have highlighted the effect of layer height on roughness of the surface in FFF-printed parts. Several investigations have emphasized the influence of layer height on the surface roughness of objects produced using FFF printing. For instance, Mushtaq et al. highlighted the importance of layer thickness in determining surface roughness [42]. Similarly, Singh et al. [43] conducted investigations using an orthogonal array and concluded that layer height was the most dominant factor influencing roughness of the surface. Furthermore, Garg et al. [44] studied the effect of layer height and part deposition orientation on roughness of the surface using an artificial neural network, further emphasizing the importance of layer thickness. Consistent with findings in some existing literature [45,46], the surface roughness positively correlated with both the temperature and time of the annealing heat treatment. On the other hand, Novotný et al. reported that thermal annealing maintained the complicated three-dimensional structure of PLA produced through 3D printing, suggesting a multifaceted connection between annealing and surface roughness [47]. The annealing process, layer height, and build orientation are all critical factors in defining the roughness of the surface of parts in FFF technology.

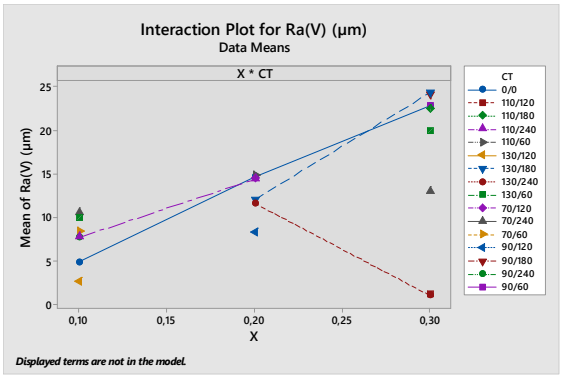

(a)

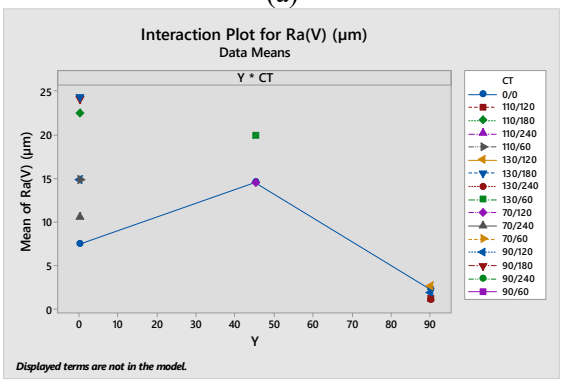

(b)

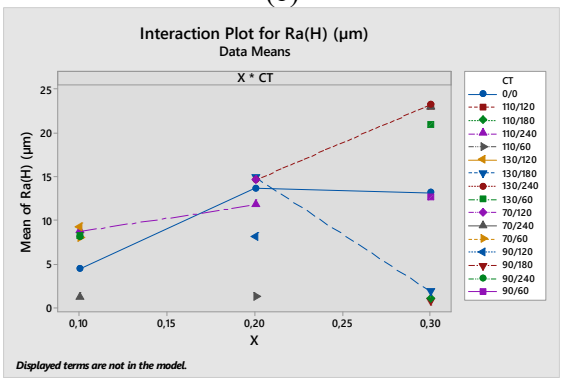

(c)

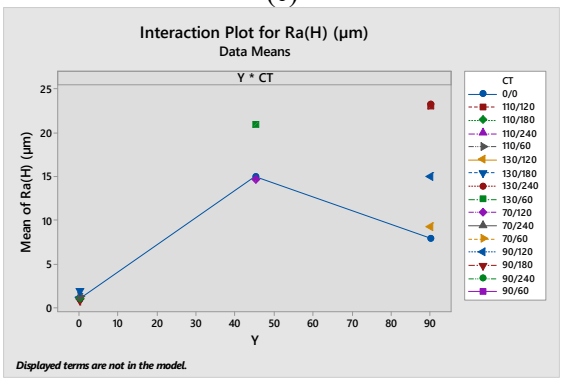

(d)

Figure 6. The surface roughness interaction plot with layer height, build orientation, and annealing parameters.

The dimensional accuracy of the dog bone tensile test specimen was determined by the proximity of the thickness and width values in a gauge zone to the CAD dimensions and the actual dimensions of the specimen. Based on the CAD measurements, the value of b should be 13 mm and the value of h should be 3.2 mm. The interaction plots demonstrating the influence of printing and annealing parameters on the values of b and h are shown in Figure 7. When analyzing the graphs, it becomes evident that the b value exhibits more dimensional precision when the build orientation is set at 90°, whereas the h value demonstrates higher dimensional accuracy at 0°. The natural tendency of molten matter to flow downward explains this phenomenon. Cojocaru et al. [48] highlight that the accuracy of 3D-printed PLA parts can be affected by alterations in material volume and the presence of residual stress resulting from PLA crystallinity. The graphs also clearly indicate that there is a greater level of dimensional precision when the layer thickness is smaller. While the annealing process parameters generally have an adverse impact on dimensional accuracy, the impact of these variables on precision in dimensions does not exhibit a linear rise. The ANOVA results also confirm this.

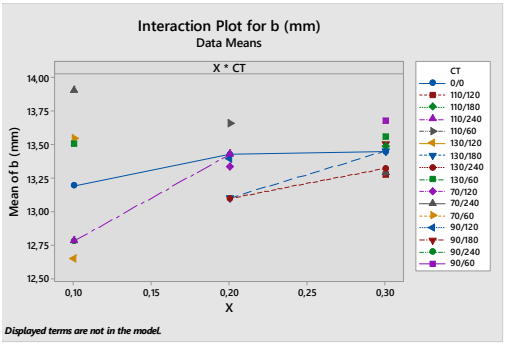

(a)

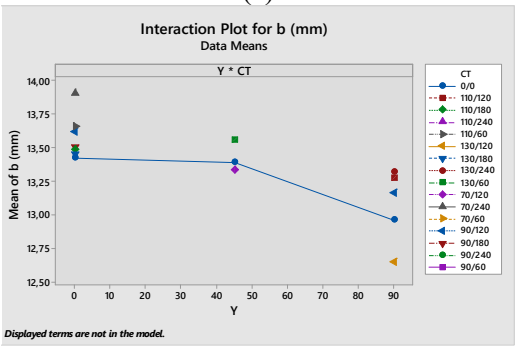

(b)

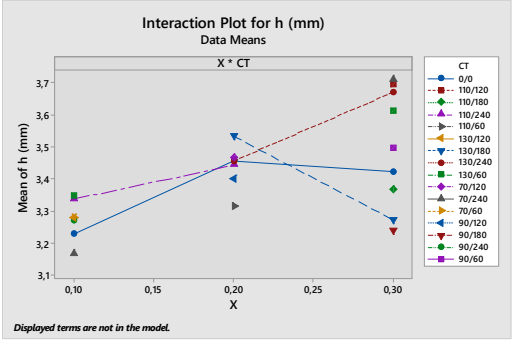

(c)

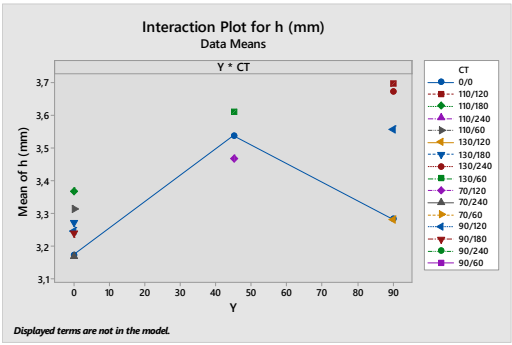

(d)

Figure 7. The dimensional accuracy interaction plot with layer height, build orientation, and annealing parameters.

The Insize ISM-PM200SA digital microscope was used to obtain macroscopic pictures of after tensile fractures, along with the previous findings. Figure 8 displays several images taken of the post-fracture specimens. Although the build orientation and layer heights are same between run 1 and run 5, the annealing process produces noticeable differences in the two samples. The sample that underwent annealing shows greater uniformity in its structure. Results from samples run 4, 8, and 17 indicate that the 90° build orientation performs better at lower layer thicknesses and lower annealing temperatures. The best results are achieved without any annealing. Furthermore, an intralayer fracture is seen on the fracture surface of sample number 4. This result indicates that the printing temperature and other printing settings for the filament are suitable. When comparing all angles, it is evident that the results improve as the angles approach zero. It becomes less effective as it nears a 90° angle. When samples with low build orientations are analyzed, samples at run 5, 9, and 13 exhibited the highest shape integrity with minimal gap between layers in low build orientations. As the building angles of the samples approach 0º, the tension in the tensile test will align with the layers of the sample being formed. Rupture occurs when the tensile stresses increase as the cross-sectional area of the layer decreases. The layers are created by stretching fibers in the direction of a pulling force and then breaking them into chopped layers.

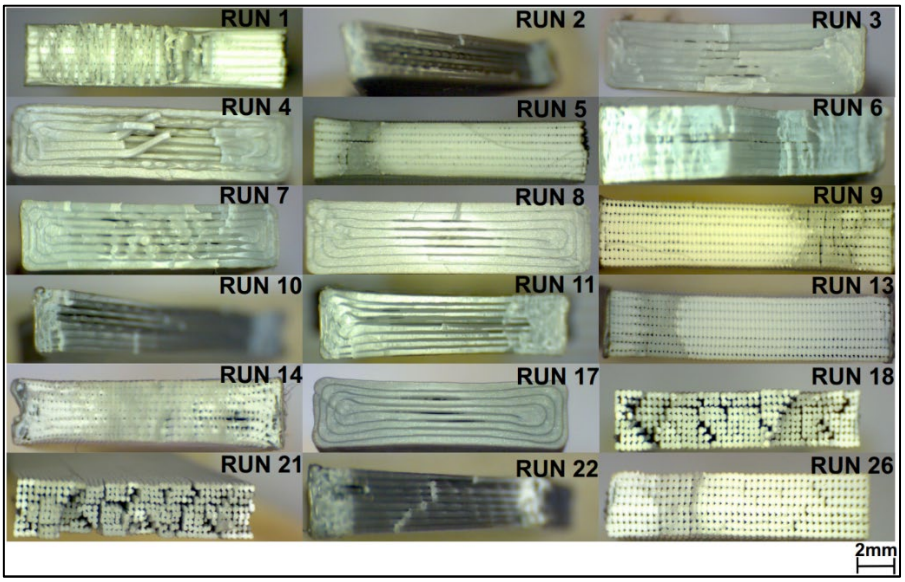

Figure 8. Microstructure of tensile specimen rupture surfaces.

An analysis of the results obtained from RSM-based multipurpose optimization is conducted as part of this investigation. The guiding principle of the optimization procedure is to minimize or maximize the output responses, which include dimensional accuracy, surface

irregularity, and UTS. The basics of optimization involve achieving dimensional accuracy, approaching the desired size, minimizing surface roughness (specifically Ra(V) and Ra(H)), and simultaneously maximizing the UTS. The RSM optimization study, shown in Figure 9 (a), determined the ideal values for the layer height, build orientation, annealing temperature, and annealing time as follows: 0.1 mm for the layer height, 0 degrees for the build orientation, 110 degrees for the annealing temperature, and 180 dk mm for the annealing time. The values of Ra(V), Ra(H), b, h, and the UTS are determined to be 7.19 µm, -2.99 µm, 13.32 mm, 3.28 mm, and 52.40 MPa, respectively, given the specified optimal variable conditions. Desirability quantifies how well a process or product metric complies with specifications using a standardized scale. The weighted geometric mean may then be used to aggregate the individual desirability evaluations into a multiresponse composite desirability score. This index gives a single numerical value for requirement conformity, making it easy to evaluate options and improve the design of a process or product.

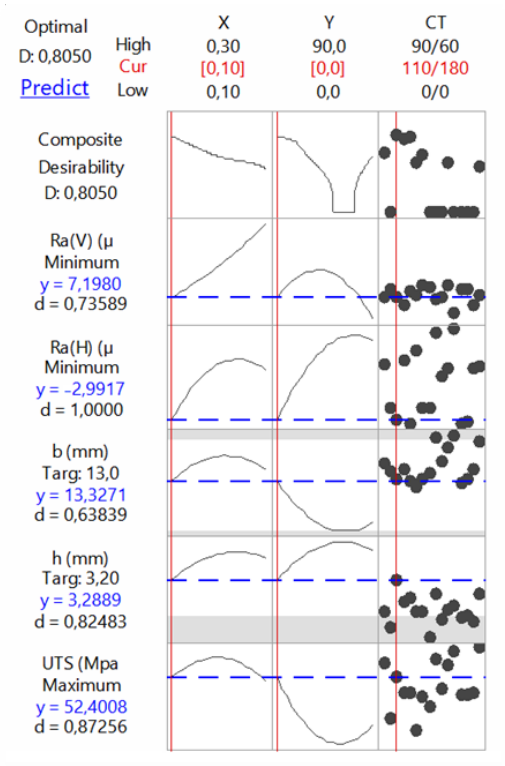

Figure 9. Predicted responses based on the best parameters for optimal results

The determined desirability levels for each response and the composite desirability are also displayed in Figure 9. The optimization investigation resulted in a composite desirability value of 0.80 for the variables. The maximum level of desirability assigned to Ra(H) is 1.0, while the minimum level of desirability assigned to b is 0.64. The corresponding levels of desirability for h, Ra(V), and UTS are 0.82, 0.73, and 0.87.Figure 10 displays surface plots illustrating the UTS, dimensional accuracy, and surface roughness based on the optimal annealing conditions.As illustrated in Figure 10, the UTS value reaches its maximum across all construction orientations when the layer height approaches 0.2 mm in the optimal annealing parameters. The parts manufactured with a 0.3 mm layer height have a minimum UTS. Additionally, the maximal UTS is observed in the 0° build direction; as the build direction increases, the UTS initially decreases and then rises around 90°. Lowering layer heights improves dimensional precision and reduces surface roughness. In accordance with the anticipated relationship, roughness of the surface is greater when measured in a direction perpendicular to the printing orientation.

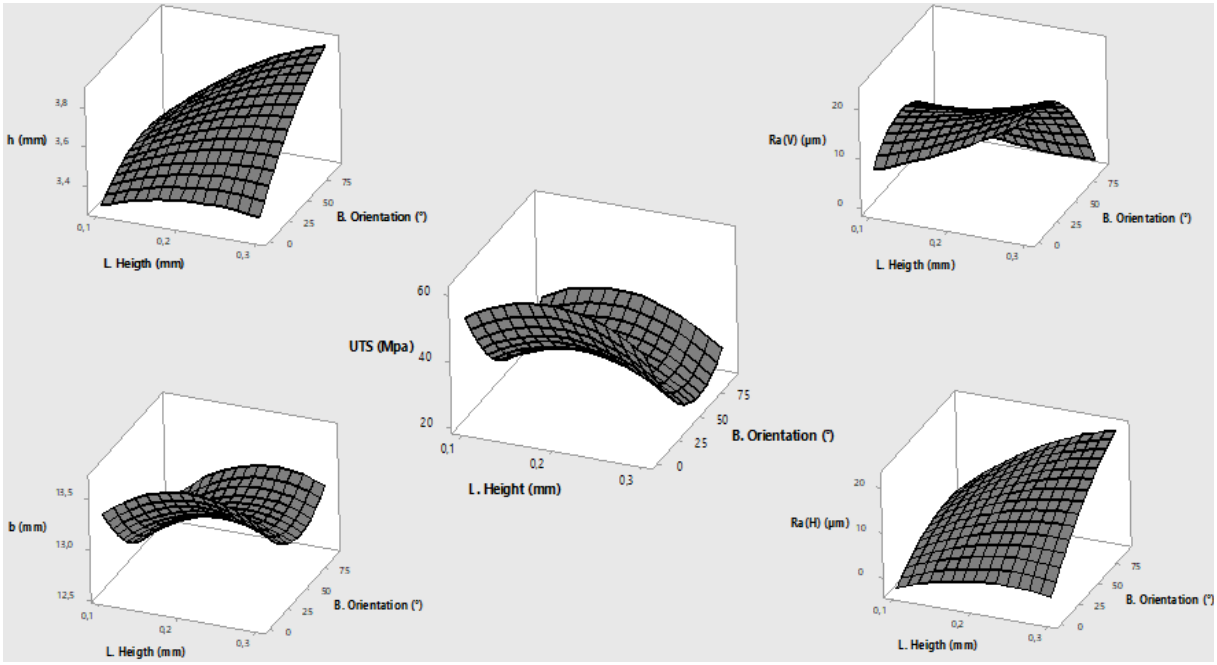

Figure 10. Surface plots displaying UTS, dimensional accuracy, and surface roughness.

The anticipated optimal results of this study were in comparison to the actual results, and the discrepancies between the two were determined. The objective of this procedure was to validate the precision and efficacy of the optimized results. Additionally, validation research was implemented in order to verify the confidence of the optimization results. The dataset for validation is presented in tabular format in Table 3. Subsequently, a comparison was performed between the experimental results acquired and the input variables' optimal values obtained through the optimization procedure. The error rates for dimensional accuracy (b and h) and UTS are notably low among all the recorded responses, falling precisely below 5%. Regarding surface roughness, the error rate in the vertical direction is 4.03%, while the error rate in the horizontal direction is considerably higher at 151.50%, suggesting a comparatively decreased degree of dependability.

Table 3 The validation results for the expected and observed values.

Build orient-ation, °	Layer height, mm	Annealing Temperature, °C	Annea-ling Time, min	Value	UTS, MPa	Ra(V)	Ra(H)	b	h
0	0.1	110	180	Anticipated	52.40	7.19	-2.99	13.32	3.28
0	0.1	110	180	Experimental	51.18	7.48	1.54	13.46	3.12
-	-	-		Error (%)	2.33	4.03	151.50	1.04	4.87

4. CONCLUSIONS

This research investigated the impact of annealing heat treatment parameters, build orientation, thickness of layers, and FFF 3D printed PLA samples on dimensional precision, mechanical characteristics, and surface roughness. The parameters for the annealing and printing were optimized by means of the response surface method. The following conclusions could be derived from the outcomes of those experiments:

- The RSM optimization resulted in an overall desirability number of 0.80, leading to optimal values for printing and annealing variables: 0° for build orientation, 0.1 mm for layer height, 110°C for annealing temperature, and 180 minutes for annealing time. The optimal variable values resulted in

responses of 7.19 μm for Ra(V), 2.99 μm for Ra(H), 13.32 mm for b, 3.28 mm for h, and 52.40 MPa for the UTS.

- The validation investigation showed that the maximum error percentage between the optimal and experimental values for UTS and dimensional accuracy was less than 5%, utilizing the printing and annealing variables determined through RSM optimization. The maximum percentage error between the optimal and experimental values exceeded 5% for surface roughness. This model's consistency with experimental data demonstrates the reliability and strong predictive capability of the established models for UTS and dimensional accuracy.
- The R2 and adjusted R2 values for each response were 96.49% and 82.44%, respectively, indicating that the model produces statistically significant results.
- The factor that has the most significant impact on all responses is the build orientation. Annealing parameters have a greater impact on the UTS compared to the layer height parameter. Annealing factors have the least influence on dimensional precision and surface roughness.
- The sample that underwent annealing exhibits not only a greater UTS value but also greater structural homogeneity and reduced volumes of voids.
- The samples with a 90° build orientation exhibit improved performance at decreasing layer thicknesses and annealing temperatures, reaching their peak performance without annealing. This occurs due to the printing temperature being ideal for this filament, resulting in strong interlayer adhesion.
- Positive outcomes were observed throughout the annealing process in samples oriented at a 0° build angle, whereas negative outcomes were noted when increasing the layer thickness. The most favorable results were attained with a thickness of 0.1 mm. Comparing all angles reveals that the closer they are to zero, the more favorable the outcomes. It becomes less effective as it nears a 90° angle.

ACKNOWLEDGMENTS AND FUNDING INFORMATION

Scientific Research Projects Coordination Unit of Karabuk University provided funding for this study. KBÜBAP-23-YL-149 is the project number. We appreciate the support.

Potential Conflicts of Interest Statement

Not a single conflict of interest exists, according to the authors.

REFERENCES

1. Ligon, S. C., Liska, R., Stampfl, J., Gurr, M., and Mülhaupt, R., "Polymers for 3D Printing and Customized Additive Manufacturing", Chemical Reviews, Vol. 117, Issue 15, Pages 10212–10290, 2017.

2. Ellson, G., Carrier, X., Walton, J., Mahmood, S. F., Yang, K., Salazar, J., and Voit, W. E., "Tough thiourethane thermoplastics for fused filament fabrication", Journal of Applied Polymer Science, Vol. 135, Issue 6, Pages 1-7, 2018.

3. El Magri, A., El Mabrouk, K., Vaudreuil, S., Chibane, H., and Touhami, M. E., "Optimization of printing parameters for improvement of mechanical and thermal performances of 3D printed poly(ether ether ketone) parts", Journal of Applied Polymer Science, Vol. 137, Issue 37, Pages 1-14, 2020.

4. Floor, J., Van Deursen, B., and Tempelman, E., "Tensile strength of 3D printed materials: Review and reassessment of test parameters", Materials Testing, Vol. 60, Issue 8, Pages 679-686, 2018.

5. Mahmood, A., Akram, T., Chen, H., and Chen, S., "On the Evolution of Additive Manufacturing (3D/4D Printing) Technologies: Materials, Applications, and Challenges", Polymers, Vol. 135, Issue 6, Pages 1-31, 2018.

6. Öz, Ö., Öztürk, F. H., and Güleç, C., "Effect of fiber content and plasticizer on mechanical and joint properties of carbon fiber powder reinforced PLA manufactured by 3D printing process", Journal of Adhesion Science And Technology, Vol. 37, Issue 15, Pages 2208-2231, 2023.

7. Çakan, B. G., "Effects of raster angle on tensile and surface roughness properties of various FDM filaments", Journal of Mechanical Science and

Technology, Vol. 35, Issue 8, Pages 3347-3353, 2021.

8. Eryildiz, M., "Comparison of notch fabrication methods on the impact strength of FDM-3D-printed PLA specimens", Materials Testing, Vol. 65, Issue 3, Pages 423-430, 2023.

9. Demir, S., Temiz, A., and Pehlivan, F., "The investigation of printing parameters effect on tensile characteristics for triply periodic minimal surface designs by TAGUCHI", Polymer Engineering & Science, Vol. 64, Issue 3, Pages 1209-1221, 2024.

10. Rajpurohit, S. R. and Dave, H. K., "Effect of process parameters on tensile strength of FDM printed PLA part", Rapid Prototyping Journal, Vol. 24, Issue 8, Pages 1317-1324, 2018.

11. Magri, A. E., El Mabrouk, K., Vaudreuil, S., and Touhami, M. E., "Mechanical properties of CF-reinforced PLA parts manufactured by fused deposition modeling", Journal of Thermoplastic Composite Materials, Vol. 34, Issue 5, Pages 581-595, 2021.

12. Vyavahare, S., Teraiya, S., Panghal, D., and Kumar, S., "Fused deposition modelling: a review", Rapid Prototyping Journal, Vol. 26, Issue 1, Pages 176-201, 2020.

13. Hua, L., Wang, X., Ding, L., Zeng, S., Liu, J., and Wu, Z., "Effects of fabrication parameters on the mechanical properties of short basalt-fiber-reinforced thermoplastic composites for fused deposition modeling-based 3D printing", Polymer Composites, Vol. 44, Issue 6, Pages 3341-3357, 2023.

14. Vyavahare, S., Kumar, S., and Panghal, D., "Experimental study of surface roughness, dimensional accuracy and time of fabrication of parts produced by fused deposition modelling", Rapid Prototyping Journal, Vol. 26, Issue 9, Pages 1535-1554, 2020.

15. Chohan, J. S. and Singh, R., "Pre and post processing techniques to improve surface characteristics of FDM parts: a state of art review and future applications", Rapid Prototyping Journal, Vol. 23, Issue 3, Pages 495-513, 2017.

16. Syrlybayev, D., Zharylkassyn, B., Seisekulova, A., Akhmetov, M., Perveen, A., and Talamona, D., "Optimisation of Strength Properties of FDM Printed Parts—A Critical Review", Polymers, Vol. 13, Issue 10, Pages 1-35, 2021.

17. Dey, A. and Yodo, N., "A Systematic Survey of FDM Process Parameter Optimization and Their Influence on Part Characteristics", Journal of Manufacturing and Materials Processing, Vol. 3, Issue 3, Pages 1-30, 2019.

18. Singh, J., Goyal, K. K., Kumar, R., and Gupta, V., "Development of artificial intelligence-based neural network prediction model for responses of additive manufactured polylactic acid parts", Polymer Composites, Vol. 43, Issue 8, Pages 5623-5639, 2022.

19. Huang, M., Zheng, N., Qin, Y., Tang, Z., Zhang, H., Fan, B., and Qin, L., "Description Logic Ontology-Supported Part Orientation for Fused Deposition Modelling", Processes, Vol. 10, Issue 7, Pages 1-20, 2022.

20. Zhiani Hervan, S., Altınkaynak, A., and Parlar, Z., "Hardness, friction and wear characteristics of 3D-printed PLA polymer", Proceedings Of The Institution Of Mechanical Engineers, Part J: Journal of Engineering Tribology, Vol. 235, Issue 8, Pages 1590-1598, 2021.

21. Eryildiz, M., "Effect of Build Orientation on Mechanical Behaviour and Build Time of FDM 3D-Printed PLA Parts: An Experimental Investigation", European Mechanical Science, Vol. 5, Issue 3, Pages 116-120, 2021.

22. Yilmaz, M. and Yilmaz, N. F., "Effects of raster angle in single- and multi-oriented layers for the production of polyetherimide (PEI/ULTEM 1010) parts with fused deposition modelling", Materials Testing, Vol. 64, Issue 11, Pages 1651-1661, 2022.

23. Akhoundi, B., Nabipour, M., Hajami, F., and Shakoori, D., "An Experimental Study of Nozzle Temperature and Heat Treatment (Annealing) Effects on Mechanical Properties of High-Temperature Polylactic Acid in Fused Deposition Modeling", Polymer Engineering & Science, Vol. 60, Issue 5, Pages 979-987, 2020.

24. Torres, J., Abo, E., and Sugar, A. J., "Effects of annealing and acetone vapor smoothing on the tensile properties and surface roughness of FDM printed ABS components", Rapid Prototyping Journal, Vol. 29, Issue 5, Pages 921-934, 2023.

25. Shbanah, M., Jordanov, M., Nyikes, Z., Tóth, L., and Kovács, T. A., "The Effect of Heat Treatment on a 3D-Printed PLA Polymer's Mechanical Properties", Polymers, Vol. 15, Issue 6, Pages 1-12, 2023.

26. Rane, R., Kulkarni, A., Prajapati, H., Taylor, R., Jain, A., and Chen, V., "Post-Process Effects of Isothermal Annealing and Initially Applied Static Uniaxial Loading on the Ultimate Tensile Strength

of Fused Filament Fabrication Parts", Materials, Vol. 13, Issue 2, Pages 1-18, 2020.

27. Elkaseer, A., Schneider, S., and Scholz, S. G., "Experiment-Based Process Modeling and Optimization for High-Quality and Resource-Efficient FFF 3D Printing", Applied Sciences, Vol. 10, Issue 8, Pages 1-18, 2020.

28. El Magri, A., El Mabrouk, K., Vaudreuil, S., and Ebn Touhami, M., "Experimental investigation and optimization of printing parameters of 3D printed polyphenylene sulfide through response surface methodology", Journal of Applied Polymer Science, Vol. 138, Issue 1, Pages 1-13, 2021.

29. Ouassil, S., El Magri, A., Vanaei, H. R., and Vaudreuil, S., "Investigating the effect of printing conditions and annealing on the porosity and tensile behavior of 3D -printed polyetherimide material in Z -direction", Journal of Applied Polymer Science, Vol. 140, Issue 4, Pages 1-16, 2023.

30. Tho, N. H., "Application of box-behnken, ann, and anfis techniques for identification of the optimum processing parameters for fdm 3d printing parts", Journal of Industrial Engineering and Halal Industries, Vol. 3, Issue 1, Pages 64-86, 2022.

31. I. ASTM, Standard Test Method for Tensile Properties of Plastics ,2022.

32. Hashmi, A. W., Mali, H. S., and Meena, A., "A comprehensive review on surface quality improvement methods for additively manufactured parts", Rapid Prototyping Journal, Vol. 29, Issue 3, Pages 504-557, 2023.

33. Temiz, A., "The Effects of Process Parameters on Tensile Characteristics and Printing Time for Masked Stereolithography Components, Analyzed Using the Response Surface Method", Journal of Materials Engineering and Performance, Vol. 1, Issue 1, Pages 1-10, 2023.

34. Cotabarren, I., Palla, C. A., McCue, C. T., and Hart, A. J., "An assessment of the dimensional accuracy and geometry-resolution limit of desktop stereolithography using response surface methodology", Rapid Prototyping Journal, Vol. 25, Issue 7, Pages 1169-1186, 2019.

35. Wang, K., Lam, F. "Quadratic RSM Models of Processing Parameters for Three-Layer Oriented Flakeboards", Wood Fiber Sci. Vol. 31, Issue 2, Pages 173-186, 1999.

36. Choudhary, N., Sharma, V., and Kumar, P., "Polylactic acid-based composite using fused filament fabrication: Process optimization and biomedical application", Polymer Composites, Vol. 44, Issue 1, Pages 69-88, 2023.

37. Moreno, R., Carou, D., Carazo-Álvarez, D., and Gupta, M. K., "Statistical models for the mechanical properties of 3D printed external medical aids", Rapid Prototyping Journal, Vol. 27, Issue 1, Pages 176-186, 2021.

38. Lanzotti, A., Grasso, M., Staiano, G., and Martorelli, M., "The impact of process parameters on mechanical properties of parts fabricated in PLA with an open-source 3-D printer", Rapid Prototyping Journal, Vol. 21, Issue 5, Pages 604-617, 2015.

39. Grasso, M., Azzouz, L., Ruiz-Hincapie, P., Zarrelli, M., and Ren, G., "Effect of temperature on the mechanical properties of 3D-printed PLA tensile specimens", Rapid Prototyping Journal, Vol. 24, Issue 8, Pages 1337-1346, 2018.

40. Wang, S., Ma, Y., Deng, Z., Zhang, S., and Cai, J., "Effects of fused deposition modeling process parameters on tensile, dynamic mechanical properties of 3D printed polylactic acid materials", Polymer Testing, Vol. 86, Issue 1, Pages 1-8, 2020.

41. Frunzaverde, D., Cojocaru, V., Ciubotariu, C.-R., Miclosina, C.-O., Ardeljan, D. D., Ignat, E. F., and Marginean, G., "The Influence of the Printing Temperature and the Filament Color on the Dimensional Accuracy, Tensile Strength, and Friction Performance of FFF-Printed PLA Specimens", Polymers, Vol. 14, Issue 10, Pages 1-15, 2022.

42. Mushtaq, R. T., Iqbal, A., Wang, Y., Cheok, Q., and Abbas, S., "Parametric Effects of Fused Filament Fabrication Approach on Surface Roughness of Acrylonitrile Butadiene Styrene and Nylon-6 Polymer", Materials, Vol. 15, Issue 15, Pages 1-25, 2022.

43. Singh, J., Singh, R., and Singh, H., "Investigations for improving the surface finish of FDM based ABS replicas by chemical vapor smoothing process: a case study", Assembly Automation, Vol. 37, Issue 1, Pages 13-21, 2017.

44. Garg, A., Bhattacharya, A., and Batish, A., "On Surface Finish and Dimensional Accuracy of FDM Parts after Cold Vapor Treatment", Materials and Manufacturing Processes, Vol. 31, Issue 4, Pages 522-529, 2016.

45. Wang, S., Daelemans, L., Fiorio, R., Gou, M., D'hooge, D. R., De Clerck, K., and Cardon, L., "Improving Mechanical Properties for Extrusion-Based Additive Manufacturing of Poly(Lactic Acid)

by Annealing and Blending with Poly(3-Hydroxybutyrate)", Polymers, Vol. 11, Issue 9, Pages 1-13, 2019.

46. Park, S.-S., Lee, Y.-S., Lee, S.-W., Repo, E., Kim, T.-H., Park, Y., and Hwang, Y., "Facile Surface Treatment of 3D-Printed PLA Filter for Enhanced Graphene Oxide Doping and Effective Removal of Cationic Dyes", Polymers, Vol. 15, Issue 2, Pages 1-19, 2023.

47. Novotný, F., Urbanová, V., Plutnar, J., and Pumera, M., "Preserving Fine Structure Details and Dramatically Enhancing Electron Transfer Rates in Graphene 3D-Printed Electrodes via Thermal Annealing: Toward Nitroaromatic Explosives Sensing", ACS Applied Materials & Interfaces, Vol. 11, Issue 38, Pages 35371-35375, 2019.

48. Cojocaru, V., Frunzaverde, D., Miclosina, C.-O., and Marginean, G., "The Influence of the Process Parameters on the Mechanical Properties of PLA Specimens Produced by Fused Filament Fabrication—A Review", Polymers, Vol. 14, Issue 5, Pages 1-23, 2022.